Presented at the 35th European PV Solar Energy Conference and Exhibition, 24-28 September 2018, Brussels, Belgium

METALLIZATION FRACTION OF BIFACIAL pSPEER SHINGLE SOLAR CELLS

M. Al-Akash, P. Baliozian, E. Lohmüller, T. Fellmeth, N. Wöhrle, R. Preu
Fraunhofer Institute for Solar Energy Systems (ISE), Heidenhofstr. 2, 79110 Freiburg, Germany
Phone: +49 761 - 4588 5011; e-mail: mohammad.al-akash@ise.fraunhofer.de

ABSTRACT: We present the investigation of metallization fraction of bifacial p-type silicon shingled passivated edge, emitter and rear (pSPEER) solar cells intended for shingled module integration. For the first group G_1 (cell dimension: 23 mm x 148 mm), ten fabricated pSPEER cells, five each with a different busbar layout (single and double busbar), are utilized to measure the contact widths and calculate the metal coverage. Taking into account the shingling interconnected cell is overlapped, the reduced and therefore designated area metallization fraction is represented by the metal coverage of fingers and redundant line. The rear side metallization fraction for G_1 for single and double busbar layouts based on designated area remain for both busbar types almost the same with around 25.9%. The same applies to the front side resulting in around 3.0%. For the second group G_2 (cell dimension: 22 mm x 148 mm), five fabricated pSPEER cells are used. Metallization fraction for this group is lower than G_1. The designated area metal coverage fraction on the rear side is 19.8%. The front side features metallization fraction of 2.8%. A complete overlap should be ensured precisely to avoid any variations in metallization fraction affecting the expected short-circuit current density values.
Keywords: Bifacial shingle cells, pSPEER, metallization fraction, designated area.

1 INTRODUCTION

Shingling solar cells are realized by overlapping the front side busbar of a cell by the rear side busbar of neighboring cell leading to a visually busbarless front and rear side of the final shingle solar module. A complete overlap, attained by entirely covering the busbar, causes a reduction in the cell area and therefore a designated area which is the difference between total cell area and overlapped cell area [1]; see Fig. 1. Shingling interconnection of bifacial shingle solar cells is an approach to increase the output power density due to the reduction of the inactive area which is covered significantly by busbars on front and rear sides. Hence, the shading metal is then replaced by its adjacent neighbor's active area being valid also for the rear side for bifacial solar cells. The overlap provides a mechanical and electrical junction to adjacent cells. In addition, shingling decreases the series resistance on the interconnection level.

The interest in shingle cell and module technology is rising. Market share of bifacial solar cells as well as shingled interconnection technology is expected to rise in the upcoming years [2]. Monofacial shingle modules are available in the market in addition to an increase in the number of publications in shingling concepts [3–5].

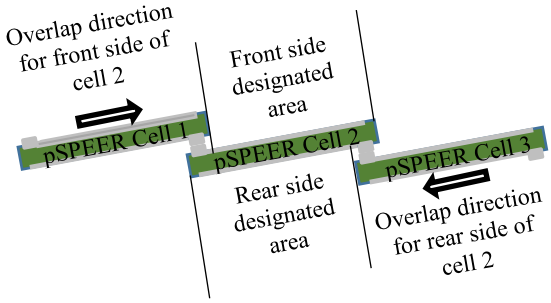

Figure 1: Labeled side-view illustration of shingled solar cells. The rear side busbar of pSPEER cell 1 overlaps the front side busbar of cell 2, whereas the rear side of cell 2 overlaps the front side of pSPEER cell 3 obtaining front and rear side designated areas of pSPEER cell 2.

The bifacial p-type silicon shingled passivated edge, emitter and rear (pSPEER) solar cells [6] are based on the p-type Czochralski-grown silicon (Cz-Si) passivated emitter and rear cell (PERC) approach. The 6-inch PERC host wafers exhibit the shingle metallization layouts on front and rear side and the single shingle cells are separated from the host wafer after contact firing. From each host wafer, six pSPEER cells are obtained.

This paper introduces a general overview of the metallization of two groups G_1 and G_2 of pSPEER solar cells with different geometries. It also investigates the change of visible metallization fraction of different overlap scenarios of pSPEER cells by taking into account scenarios meant for shingled module integration. It is crucial to examine the busbar area on both sides in order to precisely determine the overlap distance needed to maximize interconnection area and short-circuit current simultaneously.

2 METALLIZATION OF pSPEER SOLAR CELLS AND INVESTIGATION METHOD

Industrial 6-inch p-type Cz-Si PERC precursors with front and rear side dielectric passivation are used for the fabrication of pSPEER solar cells. Laser rear local contact opening is ensured by means of a pulsed infrared laser. Firstly, the metallization of the rear busbar is screen printed using a non-firing-through commercially available tabbing silver paste. Subsequently, the rear aluminum contact grid is screen printed on the local contact openings. The aluminum is connected to the priory printed silver busbar; see Fig. 2(a). Following that, a silver finger grid including busbars is screen printed on the front side. After fast firing, laser-assisted separation is used to obtain six pSPEER solar cells from each host wafer; see Fig. 2(b). For more details concerning the fabrication process, please refer to Ref. [7].

The pSPEER solar cells of the first group G_1 (cell dimension: 23 mm x 148 mm) feature single and double busbar formats, whilst the pSPEER cells of the second group G_2 (cell dimension: 22 mm x148 mm) only feature a single busbar format. Both groups feature different passivation layers. For G_1, ten fabricated pSPEER cells

after separation from their host wafers [6] are utilized to investigate the metallization coverage f_{met} by light microscopic measurements; five of them have a single busbar format, while the other five feature the double busbar format. For G_2, five fabricated pSPEER cells [7] are used to determine f_{met}.

The work flow, see Fig. 3, starts by measuring busbars, fingers, pads, and redundant lines through light microscopic images taken at different locations of the cells for each sample and each side. 40 measurements are performed at different positions of the front side for each cell, whereas rear side measurements are done at 70 different positions on each cell. The median of the measured metallization dimensions is considered to avoid any outliers. Subsequently, f_{met} is determined for each group and busbar layout for front and rear sides and, additionally, for different overlap cases. The considered overlap ranges from 0 mm to 2.9 mm from the cell edge in the direction of overlap, see Fig. 1, with increment steps of 0.1 mm. f_{met} is calculated at each point using equation 1;

$$f_{met}(\%) = \frac{\sum A_m}{A_{non\text{-}ov.}} \quad (1)$$

A_m refers to the metallization area covering active area and $A_{non\text{-}ov.}$ is the difference between total area and overlapped area.

In order to compare the results based on designed and measured dimensions, f_{met} is also determined at the same overlap points using the CAD metallization layout to observe the deviation of f_{met} based on design and measurement.

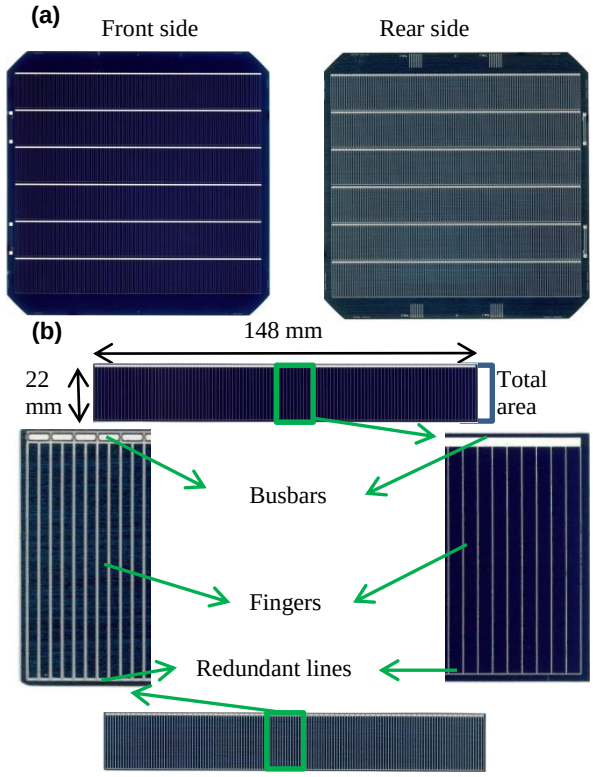

Figure 2: Photographs of (a) a host wafer of group G_2 with single busbar layout, (b) front and rear sides separated single busbar pSPEER solar cells from the G_2 host wafer. The metallization covering the active area is labeled.

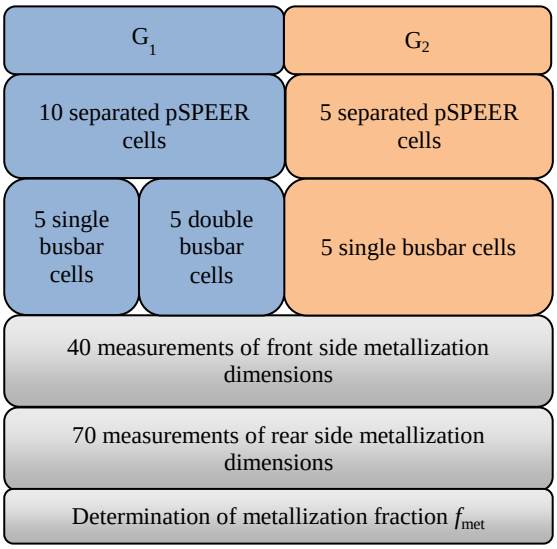

Figure 3: Flow chart of the investigation done in this work.

The rear side aluminum finger widths of the CAD layout for G_1 and G_2 are $w_{Al,rs,G1} = 250$ µm and $w_{Al,rs,G2} = 150$ µm, respectively. The rear side silver single busbar for G_1 and G_2 are $w_{Ag,rs,G1} = 600$ µm and $w_{Ag,rs,G2} = 500$ µm, respectively. For the front side, the finger width for G_1 and G_2 is designed to be $w_{Ag,fs} = 35$ µm. G_1 features a wider busbar than G_2 which reaches $w_{Ag,fs,G1} = 1300$ µm and $w_{Ag,fs,G2} = 800$ µm for G_2. The rear side redundant line of G_1 and G_2 widths are $w_{rl,rs,G1} = 100$ µm and $w_{rl,rs,G2} = 150$ µm. Whereas for the front side both groups have the same redundant line width $w_{rl,fs} = 40$ µm.

The rear side of each group and busbar layout has higher f_{met} than the front side due to the wider finger contacts on the rear side. In addition, the rear side has more fingers since the finger pitch is lower compares to the front side. Both groups have 148 fingers on the rear side. The front side of G_1 has 100 fingers compared to 114 fingers for G_2. The rear side of G_2 features lower f_{met} than the rear side of G_1 based on the finger width mentioned before.

3 RESULTS AND DISCUSSION

3.1 Measured metallization dimensions of pSPEER cells

The measured metallization dimensions on the rear and front side of each busbar layout for G_1 and G_2 is shown in Table I. In addition, the standard deviation is calculated. The standard deviation of metallization dimensions on the rear side of G_2 is higher than G_1. This can be explained due to using precursors with different rear surfaces causing a different paste spreading for both groups affecting contact geometry.

3.2 f_{met} based on design and measurements

The metal coverage differs based on designed or measured metallization dimensions, see Table II. Where f_{met} is calculated using $f_{met,tot}$ referring to the total cell size, whereas it is defined as designated area $f_{met,des}$ referring to the non-overlapped area after complete overlap of the busbars; see Fig. 5. $f_{met,des}$ of G_1 for the double busbar decreases less than for the single busbar layout, due to the existence of active area between each

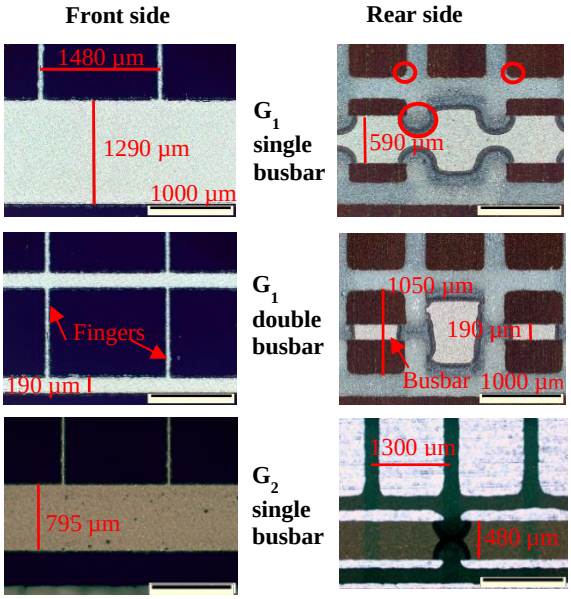

Figure 4: Microscopic images illustrating measured metallization dimensions of front and rear sides of pSPEER cells for both generations with each busbar layout. The rear side features a higher f_{met}. The aluminum fingers on the rear side smudges through the silver busbar at joining points. The highlighted joining points of fingers on the rear side feature a curved shape; however, its effect on f_{met} is negligible.

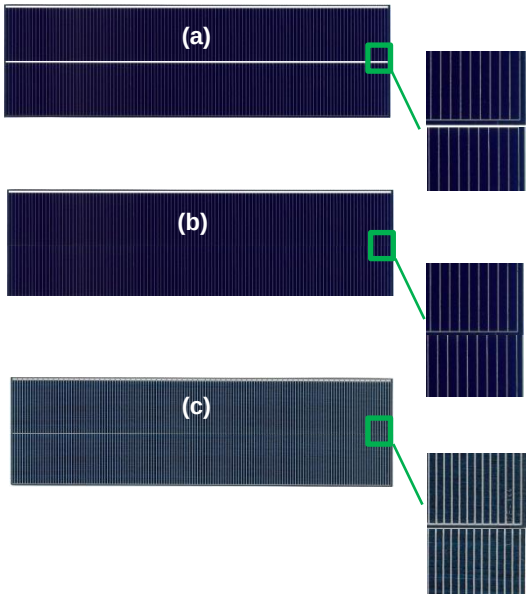

Figure 5: Photographs of (a) front side of single busbar pSPEER cells from G_2 after partial overlap, (b) front side of single busbar pSPEER cells after complete overlap and (c) rear side of single busbar pSPEER cells after complete overlap. Complete overlap from an adjacent cell is depicted to observe metallization coverage.

busbar on the front side and narrower busbar on the rear side. For G_1, the difference between f_{met} based on design and measured does not exceed 1%, while for G_2, it exceeds 4%. After taking the median of measured values, the single busbar finger width of the rear side based on measured data for G_1 and G_2 is $w_{Al,rs,G1} \approx 260$ µm and $w_{Al,rs,G2} \approx 195$ µm, respectively. The front side for G_1 and G_2 features a finger width of $w_{Ag,fs,G1} \approx 43$ µm and $w_{Ag,fs,G2} \approx 35$ µm, respectively.

3.3 f_{met} dependency on overlap

Taking into account the median of the metallization dimensions, f_{met} is calculated for each group. The rear side of G_1 pSPEER cells has higher $f_{met,rs}$ than the rear side of cells of G_2 mainly due to the wider fingers, see Fig. 6. While $f_{met,des}$ is determined after a complete overlap by entirely covering the busbar meant for shingled module integration as shown in the graph when f_{met} is at minimum and remains constant. After a complete overlap, the double busbar cell has lower f_{met} than the single busbar cell due to the existence of active area between each busbar on the front side, in addition to narrower busbar on the rear side compared to the single busbar. After a complete overlap, the metal coverage of the designated area is represented by the fingers area. Single and double busbar layouts of each side feature almost the same $f_{met,des}$, due to the similar finger width. A complete overlap is defined for each case in Table III. The curve shape of f_{met} vs overlap of each case is dependent on the metallization layout. Complete overlap should be precise when interconnecting shingle modules since a small variation of overlap before a complete overlap results in higher f_{met} resulting in lower short-current density. To point out the importance of precise complete overlap, two cases are considered.

Table I: Measured metallization dimensions for both groups with each busbar layout of front and rear sides of pSPEER cells. Dimensions are measured through light microscopic images.

Gr.	Busbar layout	Meas. side	Finger width (µm)	Standard deviation (µm)	Finger pitch (µm)	Standard deviation (µm)	Busbar width (µm)	Standard deviation (µm)	Redundant line width (µm)	Standard deviation (µm)
G_1	Single	Front	43	4.0	1480	3.2	1290	11.3	43	6.0
		Rear	260	9.6	1010	9.4	590	10.8	180	5.2
	Double	Front	41	2.5	1480	2.7	(x2) 190	14.4	41	2.5
		Rear	260	8.1	1005	6.5	190	11.1	180	8.5
G_2	Single	Front	35	2.3	1300	2.9	795	9.5	40	2.8
		Rear	195	13.8	1005	4.0	480	11.1	210	14.2

Table II: Metallization fraction of total $f_{met,tot}$ defined as f_{met} before overlap and designated area $f_{met,des}$ defined as f_{met} after complete overlap by entirely covering the busbar for both generations of front and rear sides with different busbar layouts. f_{met} is calculated using equation 1.

Gr.	Busbar layout	Meas. side	$f_{met,tot}$ based on design (%)	$f_{met,tot}$ based on meas. (%)	$f_{met,des}$ based on design (%)	$f_{met,des}$ based on meas. (%)
G_1	Single	Front	7.9	8.3	2.5	3.0
		Rear	28.4	29.2	25.0	25.9
	Double	Front	4.1	4.4	2.5	2.9
		Rear	27.1	28.1	25.1	25.9
G_2	Single	Front	6.2	6.2	2.8	2.8
		Rear	18.1	22.5	15.4	19.8

The first case is to show the effect of overlap deviation by 0.5 mm from the complete overlap for G_1 of the rear side single busbar. The complete overlap for this case is 1.9 mm from the cell edge, measured $f_{met,des} \approx 25.9\%$. Assuming an overlap deviation of 0.5 mm causing an overlap of 1.4 mm with $f_{met} \approx 26.8\%$, resulting in $\Delta f_{met} \approx 0.9\%_{abs}$. The second case is realized by applying the same but on the rear side single busbar of G_2. The complete overlap is 1.3 mm with $f_{met,des} \approx 19.8\%$. After an assumed overlap deviation of 0.5 mm, the new overlap is 0.8 mm with $f_{met} \approx 21.4\%$, resulting in $\Delta f_{met} \approx 1.6\%_{abs}$.

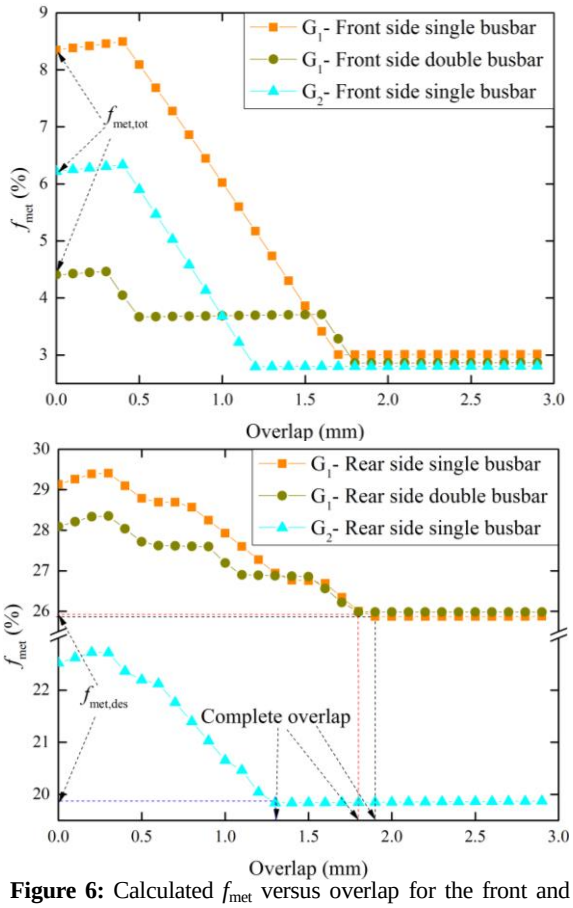

Figure 6: Calculated f_{met} versus overlap for the front and rear sides from the cell edge of each group and busbar layout. $f_{met,tot}$ is when the case of no overlap while $f_{met,des}$ is defined when f_{met} is at minimum which is shown after a complete overlap.

Table III: Complete overlap from the cell edge for both generations with each busbar layout of front and rear sides of pSPEER cells based on measured dimensions. The corresponding f_{met} is $f_{met,des}$.

Gr.	Busbar layout	Meas. side	Complete overlap (mm)
G_1	Single	Front	1.7
		Rear	1.9
	Double	Front	1.8
		Rear	1.8
G_2	Single	Front	1.2
		Rear	1.3

4 CONCLUSION AND OUTLOOK

We provide an overview of applied metallization layouts for bifacial p-type silicon shingled passivated edge, emitter and rear (pSPEER) solar cells meant for shingled module integration at Fraunhofer ISE. The study shows the determined metallization fraction before overlap $f_{met,tot}$ and after complete overlap $f_{met,des}$ for two different groups of pSPEER solar cells: group G_1 with an area of 23 mm x 148 mm and G_2 with an area of 22 mm x 148 mm. Before a complete overlap, different considered overlap cases show that a small variation of overlap causes a significant change in metallization fraction. Hence, the intended overlap needed for shingle module interconnection should be precise to avoid any changes in visible f_{met}.

For G_1, after a complete overlap and therefore a designated area, $f_{met,des}$ for single and double busbar layout of each side is almost the same, as the active area is covered only fingers and redundant line. It reaches a front $f_{met,G1,fs,des}$ around 3.0% compared to rear side $f_{met,G1,rs,des}$ of around 25.9%.

For G_2, the metallization layout is represented only by a single busbar format. After a complete overlap, f_{met} for the rear and front sides is determined to be $f_{met,G2,rs,des}$ = 19.8% and $f_{met,G2,fs,des}$ = 2.8%, respectively.

ACKNOWLEDGEMENTS

The authors would like to thank their colleagues at Fraunhofer ISE who contributed to this work. This work is supported by the German Federal Ministry of Economic Affairs and Energy within the research project "PV-BAT400" (contract no. 0324145).

REFERENCES

[1] M. A. Green, K. Emery, D. L. King, and S. Igari, "Solar cell efficiency tables (Version 15)," *Prog. Photovolt: Res. Appl.*, vol. 8, no. 1, pp. 187–195, 2000.

[2] ITRPV, "International Technology Roadmap for Photovoltaic", 2017 Results, 2018.

[3] D. Tonini, M. Bertazzo, A. Fecchio, M.Galiazzo, Ed., *Shingling Technology for Cell Interconnection: Technological Aspects and Process Integration*, 33rd ed., 2017.

[4] "'Shingle cell' P-Series solar panel from SunPower maximizing polysilicon efficiencies,"

[5] H. Gochermann and J. Soll, "Shingle-type solar cell generator prodn. - allowing formation of curved or domed product," DE3942205C2, Germany 3942205, Feb 1, 1996.

[6] P. Baliozian *et al.*, "Bifacial p-Type Silicon Shingle Solar Cells − the "pSPEER" Concept," *Sol. RRL*, vol. 55, p. 1700171, 2018.

[7] P. Baliozian, N. Wöhrle, E. Lohmüller, T. Fellmeth, R. Preu, Ed., *Bifacial shingle pSPEER solar cells for shingle modules*, 35th ed., 2018.